

Enhancing Gain in Non-Hermitian Photonic Crystals with Lossy Topological Defects

Daniel Cui¹ and Aaswath P. Raman^{1,*}

¹*Department of Materials Science and Engineering,
University of California, Los Angeles, Los Angeles, CA 90095, USA*

We show that purely lossy defects in one- and two-dimensional non-Hermitian photonic crystals can enable a dramatic gain enhancement not accessible with lossless defects. We further show that the underlying mechanism behind the loss-induced enhancement is due to the resonances being located specifically at topological branch cut phase singularities with nontrivial winding numbers. Additionally we show that these resonances behave as quasi-bound states in the continuum with exceptionally high quality factors $\sim 10^5$ or higher accessible. Our work highlights the counterintuitive role of loss in enhancing gain in non-Hermitian systems and its connection to topological phenomena in photonic systems.

Photonic structures have been widely used to enhance nonlinear optical response, improving gain and enabling high quality factors. In conventional photonic crystals, coherent effects enabled by tuning material parameters such as thickness and permittivity can lead to characteristic resonances and stop bands that are widely exploited for devices, including distributed feedback lasers [1]. Lossless defects in photonic crystals have additionally been shown to localize particular modes either within the photonic crystal bandgap [2] or within the continuum of states as a BIC [3], with resonant enhancement being exploited for a range of applications.

Recent advances in non-Hermitian photonic systems have further demonstrated that judicious arrangements of gain and loss can access new behaviors of relevance to many optical device applications. Parity-time symmetric systems [4, 5] and the observation of exceptional points [6, 7] in the photonic bandstructure have been observed due to non-Hermitian Hamiltonians being able to host real spectra and the coalescence of their associated eigenstates [5]. Such behavior is unique to such systems and not present in their Hermitian counterparts.

* aaswath@ucla.edu

New applications have also leveraged these novel phenomena and unique combinations of gain and loss systems in PT-symmetric lasers [8, 9] and in photonic integrated circuits [10]. Enhancement of emission in nonreciprocal systems [11, 12] and Anderson localization in disordered photonic systems [13, 14] have also benefited from non-Hermitian architectures. While the role of defects has been investigated in non-Hermitian photonic systems, including non-Hermitian photonic crystals, the role of lossy defects in such systems has not been explored.

In this context, we note that new frameworks have also been introduced to describe the underlying physical mechanisms behind the nontrivial phenomena observed in Non-Hermitian photonic systems. In particular topological invariants including the Chern number, global Berry phase [15], and integer winding numbers have provided insights into nontrivial photonic bandstructure topology [16] and their implications on how they affect bound states in the continuum (BICs) [17–20], exceptional points and their higher dimensional generalizations [21, 22], as well as coherent perfect absorption phenomena [23–25].

In this letter, we show that lossy defects in non-Hermitian photonic crystals result in singular behavior of their associated spectral response functions [26]. In particular, instead of acting like undesirable absorption, we demonstrate that a lossy defect placed in a non-Hermitian photonic crystal can induce multiple orders of magnitude enhancement in gain compared to the pure periodic system without loss. We characterize the nature of this phenomenon using the integer winding number of the complex reflection phase, finding that peak gain values occur precisely at the point of a topological phase transition in the system. We further generalize this behavior to a 2D non-Hermitian photonic crystal system, demonstrating that the loss-enhanced resonances in the 1D and 2D systems are both fundamentally symmetry-protected quasi-BIC's and attain very high quality factors at the topological phase transition point.

We begin by considering a model one-dimensional periodic non-Hermitian photonic crystal system. In this system, 51 unit cells, each of length a , consist of a lossless layer of length $0.8a$ and permittivity $\varepsilon_a = 2$, and a gain layer of length $0.2a$ with permittivity $\varepsilon_b = 2 - 0.1i$ (Fig. 1(a) top). When examining the reflection and transmission spectrum of this baseline periodic system, as calculated by the Transfer Matrix Method, we find a sharp resonant peak in the gain spectrum, reaching a maximum value of $\sim 10^4$ (Fig. 1(b)). We next examine the role of a centrally placed defect on enhancing the gain response of the system. In particular

we consider a lossy point defect of thickness c and complex permittivity $\epsilon_c = 2 + \epsilon_c'' * i$ where ϵ_c'' denotes the magnitude of the imaginary permittivity. The defected structure is constructed to be C_2 symmetric about the center of the defect with 25 unit cells on either side of the lossy defect.

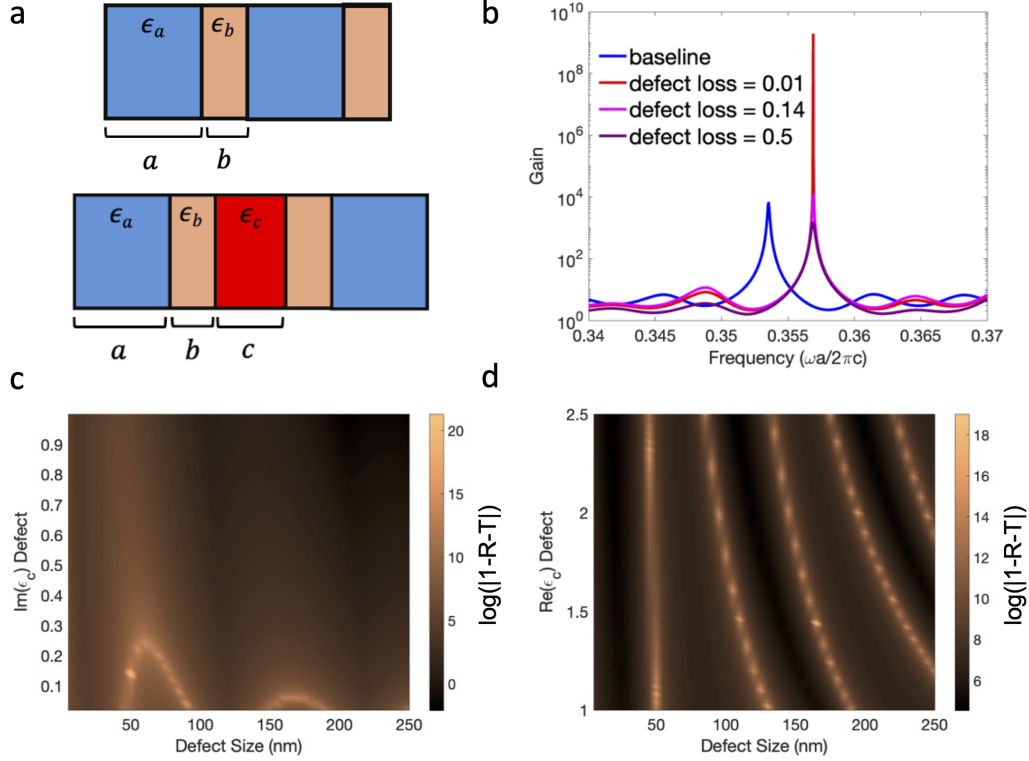


FIG. 1. (a) Schematics of the baseline periodic and defected 1D non-Hermitian photonic crystals on the top and bottom respectively. The baseline periodic system has 51 unit cells of length d of lossless $\epsilon_a = 2$ with length $a = 0.8*d$ and gain layers of $\epsilon_b = 2 - 0.1i$ with length $b = 0.2*d$. The defected structure is C_2 symmetric about the center of the lossy defect layer of $\epsilon_c = 2 + \epsilon_c'' * i$ with length c . 25 unit cells of the original baseline periodic system are located on the left of the defect. Those 25 unit cells on the left are then reflected across the center of the defect to create the right half of the structure. (b) Gain as measured by $|1 - R - T|$ for the baseline periodic structure, defected system at a loss value of 0.01, defected system at the critical defect loss value of 0.14, and defected system at a defect loss value of 0.5. (c), (d) Color plots of the maximum gain achieved in the defect structure by sweeping defect loss vs defect size on the left and $\text{Re}(\epsilon_c)$ of the defect vs defect size on the right respectively. The maximum gain is achieved when the defect is lossy and is at a loss value of 0.14.

As shown Fig. 1(b), peaks in the gain can be found within $\frac{\omega a}{2\pi c}$ of 0.34 to 0.37 for both the baseline system and the defected structures for a defect thickness of $0.5a$ where a is the unit cell length of the baseline periodic system. As the strength of the loss in the defect layer, ϵ_c'' , is increased the gain is enhanced several orders of magnitude to $> \sim 10^8$ before

then decreasing in value, suggesting that an optimal value of the loss in the defect causes a singularity-like peak in gain. To better explore this phenomenon we scanned across values of both the defect loss as well as layer thickness (Fig. 1(c)). Bands of high gain values show an unusual character, with optimal loss values existing for a given defect layer size. To contrast this against a conventional approach to defects in photonic crystal architecture, we also calculate the effect of a lossless point defect layer identically placed to the lossy defect layer (Fig. 1(d)). The resulting ranges of values for permittivity and layer thickness are consistent with a typical coherent interference effect. However, we note that using a lossy defect not only produces a larger gain enhancement than a lossless approach, but the fundamental character of maximal gain values follows a distinct pattern.

In order to elucidate the physical phenomenon behind the unique capabilities of lossy defects to induce gain enhancement, we turn to examining the phase of the complex reflection coefficient as it varies with frequency. In particular the reflection phase is taken to be $\arg(T_{11}^{TE})$ where T_{11}^{TE} is the complex reflection coefficient in the TE polarization. This then allows us to calculate a winding number for this system, following analogous approaches to characterizing the topological properties of bound state in the continuum [27], exceptional points [28], coherent perfect absorption, the Su-Schrieffer-Heeger model of the topological phases of polyacetylene [29–31], and topological defects in the XY model of spins [32, 33]. We use the following formulation of the integer winding number:

$$C = \frac{1}{2\pi} \oint d\phi, C \in \mathbb{Z} \quad (1)$$

where ϕ is the complex reflection coefficient as defined above and the convention for the path taken for line integration is taken in the direction of increasing reflection phase. In most regions of frequency space, the winding number assumes a trivial value due to there being a completely continuous definition of $\arg(T_{11}^{TE})$. In the presence of singularities however, the winding number can take on nontrivial integer values.

By modulating the loss ε_c'' in the defect of the 1D system while keeping the real part of ε_c , we observe a nontrivial winding number (Fig. 2(a)). As shown in both the complex reflection phase color plot and the slices of the color plot at various magnitudes of loss in Fig. 2(b), the complex reflection phase is discontinuous and singular up to a loss value of 0.14. Beyond 0.14, the complex reflection phase becomes continuous, indicating the presence of a

branch cut singularity. Taking an anticlockwise 2π phase loop around the branch cut, the winding number takes on a value of $+1$ which is a nontrivial value of the topological charge C of the system. Furthermore, it is important to note that the point at which the phase singularity becomes continuous at a loss value of 0.14 is also precisely the point where the gain is maximized in Fig. 1(c). At loss values beyond this critical point, the gain decreases. Thus, the gain resonance is topologically protected and remains so until a topological phase transition is made from the singular to non-singular regions of the frequency vs $Im(\varepsilon_c)$ parameter space as indicated by the winding number changing from a nontrivial $C = +1$ to trivial $C = 0$ transition (Fig. 2(a)).

By contrast, modulating the $Re(\varepsilon_c)$ without any loss in the defect leads to very different behavior. In particular, as seen in the color plot in Fig. 2(b) and the slices at various defect loss values (Fig. 2(d)), the phase is completely discontinuous. Thus, no continuous integration path exists for suitably defining the integer winding number in equation 2 and, consequently, no topological phase transition can be found in this case. The role of $Re(\varepsilon_c)$ in the defect is in stark contrast to the role of $Im(\varepsilon_c)$; in the latter, a topological phase transition as defined by nontrivial value of C is induced by the defect loss whereas the modulation of the former lacks such a transition.

We now consider an analogous two-dimensional non-Hermitian system. The baseline periodic 2D non-Hermitian photonic crystal contains of 51 unit cells that repeat in the x direction of rods surrounded by air similar to the 1D baseline periodic structure (Fig. 3(a)). Within each unit cell, there is one lossless rod of $\varepsilon_a = 2$ and a rod with gain of $\varepsilon = 2 - 0.1i$. The lossless rod has radius $r_a = 0.2a$ while the gain rod has radius $r_b = 0.1a$ where a is the unit cell length. It is also important to note that, though the photonic crystal is finite in the x -direction, Floquet periodic boundary conditions are imposed to make the system infinitely periodic in the y -direction as well. In the defected case, a geometry similar to the 1D point-defected structure is used where 25 unit cells surround either side of a lossy or lossless defect rod defined by a permittivity $\varepsilon_d = \varepsilon'_d + \varepsilon''_d i$ and radius $r_d = 0.3a$, resulting in the same C_2 symmetry as the 1D system. Since Floquet periodic boundary conditions were placed on the boundaries in the y -direction, a line defect is created instead of a point defect in this system. 4a.

As in the 1D system, increasing the loss in the point defect up to a critical value leads to multiple orders of magnitude in gain enhancement Fig. 3(b). This behavior can be

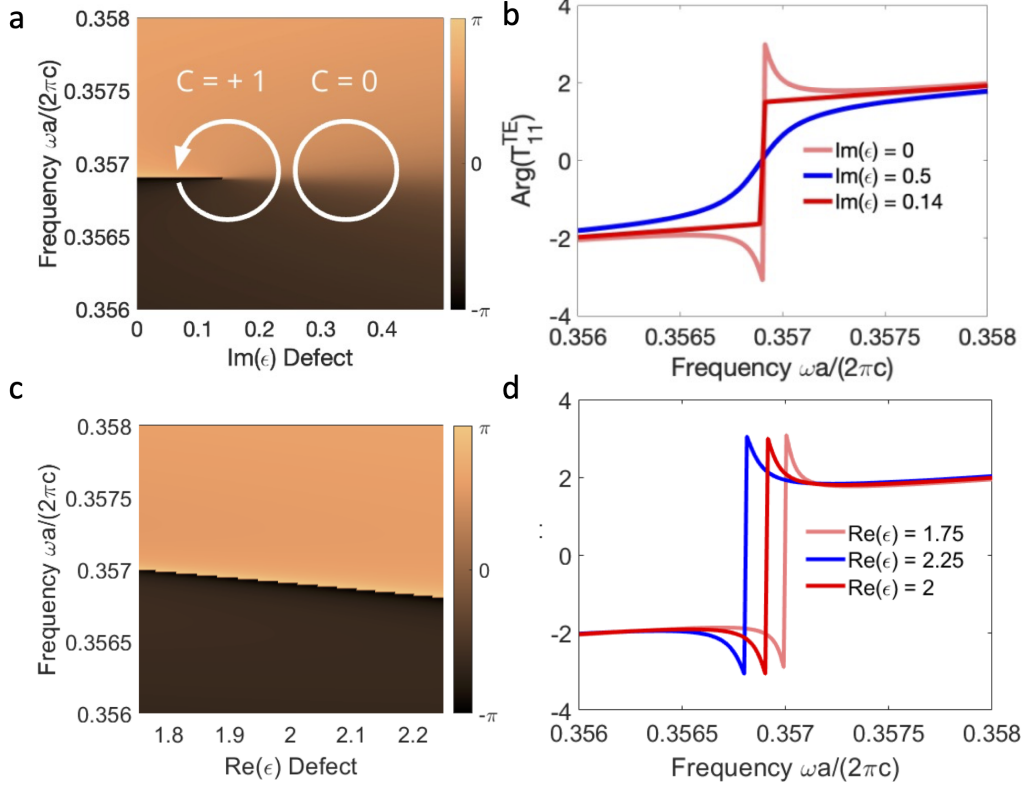


FIG. 2. (a) The complex reflection phase plotted over $\text{Re}(\omega) * a/(2\pi c)$ where a is the unit cell length and c is the speed of light vs defect loss on the left and cross sections of the color plot at various defect loss values on the right. A branch cut singularity appears starting at $\epsilon_c'' = 0$ and goes until $\epsilon_c'' = 0.14$ after which the complex reflection phase is no longer singular. The branch cut singularity also has a topological charge of $C = +1$. (b) The complex reflection phase plotted over $\text{Re}(\omega)a/(2\pi c)$ vs $\text{Re}(\epsilon_c)$ of the defect without any defect loss with color plot on the left and cutlines on the right. The complex reflection phase exhibits a discontinuity for all values of $\text{Re}(\epsilon_c)$.

understood by examining the integer winding of the complex reflection phase in the frequency vs ϵ_d parameter space. Modulating the loss, as shown in Fig. 4(a), within the defect induces a topological phase transition around a critical loss value of $\epsilon_d'' = 1.5$ (while maintaining $\epsilon' = 2$) as a transition from a nontrivial winding number of $C = +1$ to a trivial winding number of $C = 0$. This is due to the presence of a branch cut phase singularity where the transition point from nontrivial to trivial winding is where the gain enhancement is at a maximum (Fig. 4(b)). By contrast, changing only the real part ϵ_d' does not induce any phase transition as the complex reflection phase is completely continuous throughout the frequency range of interest (Fig. 4(c) and 4(d)). Thus, we see again that the loss-induced gain enhancement from the line defect is due to the topological protection of the gain resonance as inferred from the integer winding number as the topological invariant.

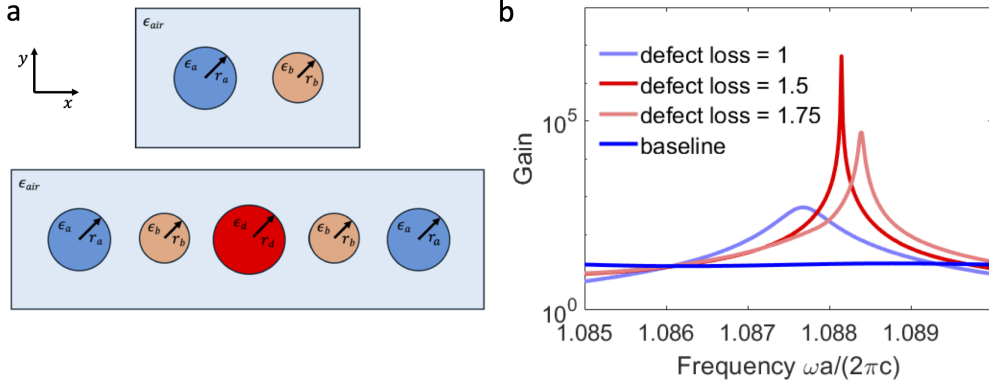


FIG. 3. (a) schematics of the baseline periodic and line-defected 2D non-Hermitian system. The baseline periodic system is shown on the right with 51 unit cells of length a . Each unit cell is surrounded by air and composed of a lossless rod of $\epsilon_a = 2$ and gain rod of $\epsilon_b = 2 - 0.1i$ with radii $0.2a$ and $0.1a$ respectively. While the photonic crystal is finite in the x direction, it is infinitely periodic in the y direction from imposing floquet periodic boundary conditions. The defected case is shown on the right which contains a lossy line defect composed of rods with ϵ_d and radius $r_d = 0.3 * a$. The defect is surrounded by 25 unit cells of the baseline periodic system on the left and right extents. (b) Gain vs frequency plots of the baseline periodic crystal compared against the lossy line defected case at loss values of 1, 1.5, and 1.75.

To provide a clearer understanding of the nature of these loss-enhanced resonances in the 1D and 2D systems, we turn to examining the location of the resonance frequency in relation to the photonic bandstructures of the baseline periodic geometries in 1D and 2D respectively. Focusing just on the real part of the bandstructure as the system is inherently non-Hermitian, the real part of the resonance frequency lies within the continuum in the periodic baseline. Doing the same calculation of the bandstructure in the reciprocal space of the 2D system, one can again see that the defect state lies within the continuum of states in the baseline bandstructure. Consequently, this shows that the loss-enhanced resonances observed in both systems have characteristics we associated with quasi-BIC's due to their finite linewidth [34].

Examination of the field profiles and quality factors as measured by $\omega_{res}/FWHM$ where the denominator is the full width half max of the resonance peak further characterizes the behavior of the quasi-BIC's. In the 1D case at the resonance peak in Figure 1(b), the field profiles of the TE field at a defect loss value of 0.14 is maximally localized at the center of the point defect. This creates a spatially symmetric mode profile that is protected by the underlying C_2 symmetry of the system. The quality factor Q is also maximized at this value of loss as well at a very high value of about 4.5×10^4 (Fig. 5(a)). This behavior can also be

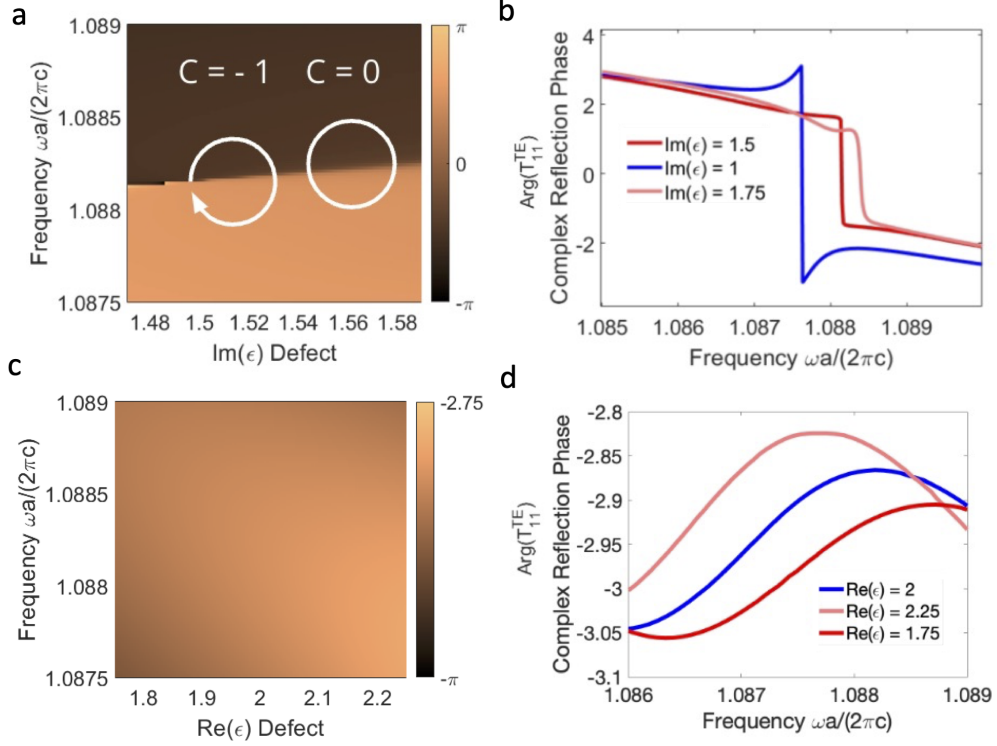


FIG. 4. (a), (b) Complex reflection phase as quantified by $\text{Arg}(TE_{11}^{TE})$ vs $\text{Im}(\epsilon_d)$ at a $\epsilon'_d = 2$ and $\text{Re}(\epsilon_d)$ at 0 loss of the line defect respectively. Increasing $\text{Im}(\epsilon_d)$ leads to a transition from a winding number of +1 to 0, while the complex reflection phase remains continuous with changing $\text{Re}(\epsilon_d)$.

seen in the 2D system (Fig. 5(b)) as well the mode profile at the optimal loss value of 1.5 leads to a symmetry protected quasi-BIC about the center of the line defect. At this defect loss value, the Q factor is also maximized as well reaching to a value $\sim 10^5$ (Fig. 5(b)).

In summary, we have demonstrated that material loss, in contrast to the material's real part of its permittivity can play the unexpected role of enhancing gain through a topological phase transition in 1D and 2D non-Hermitian photonic crystals. These resonances are additionally quasi-BIC's whose Q factors reach maximal values at the point of the phase transition. Our work highlights different the role that material loss and defects can play in non-Hermitian photonic structures. More broadly, it highlights how phase singularities can be used to engineer nonlinear photonic systems to have exceptional performance.

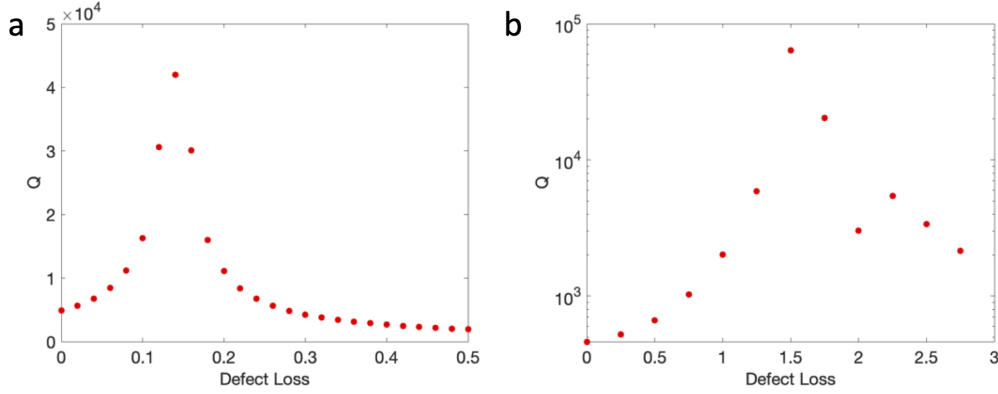


FIG. 5. (a) Q factor of the quasi-BIC in the 1D system. At the defect loss value of 0.14 the resonance attains a maximum Q. (b) Q factor of the quasi-BIC in the 2D system. It should be noted that the y-axis of the Q factor vs defect loss plot is on a logarithmic scale.

I. ACKNOWLEDGMENTS

This material is based upon work supported by the National Science Foundation under grants No. ECCS-2146577 and CBET-2401080.

-
- [1] M. L. M. Larry A. Coldren, Scott W. Corzine, Mirrors and resonators for diode lasers, in *Diode Lasers and Photonic Integrated Circuits* (John Wiley & Sons, Ltd, 2012) Chap. Three, pp. 91–155, <https://onlinelibrary.wiley.com/doi/pdf/10.1002/9781118148167.ch3>.
 - [2] J. D. Joannopoulos, S. G. Johnson, J. N. Winn, and R. D. Meade, *Molding the flow of light*, Princeton Univ. Press, Princeton, NJ [ua] (2008).
 - [3] S. Vaidya, W. A. Benalcazar, A. Cerjan, and M. C. Rechtsman, Point-defect-localized bound states in the continuum in photonic crystals and structured fibers, *Phys. Rev. Lett.* **127**, 023605 (2021).
 - [4] Ş. K. Özdemir, S. Rotter, F. Nori, and L. Yang, Parity–time symmetry and exceptional points in photonics, *Nature materials* **18**, 783 (2019).
 - [5] C. M. Bender and S. Boettcher, Real spectra in non-hermitian hamiltonians having p t symmetry, *Physical Review Letters* **80**, 5243 (1998).
 - [6] H. Zhou, J. Y. Lee, S. Liu, and B. Zhen, Exceptional surfaces in pt-symmetric non-hermitian photonic systems, *Optica* **6**, 190 (2019).

- [7] A. Mostafazadeh, Spectral singularities of complex scattering potentials and infinite reflection and transmission coefficients at real energies, *Phys. Rev. Lett.* **102**, 220402 (2009).
- [8] H. Hodaei, M.-A. Miri, M. Heinrich, D. N. Christodoulides, and M. Khajavikhan, Parity-time-symmetric microring lasers, *Science* **346**, 975 (2014).
- [9] E. Şeker, B. Olyaeefar, K. Dadashi, S. Şengül, M. H. Teimourpour, R. El-Ganainy, and A. Demir, Single-mode quasi PT-symmetric laser with high power emission, *Light: Science & Applications* **12**, 149 (2023).
- [10] E. L. Pereira, H. Li, A. Blanco-Redondo, and J. L. Lado, Non-hermitian topology and criticality in photonic arrays with engineered losses, *Phys. Rev. Res.* **6**, 023004 (2024).
- [11] J. Zhong, K. Wang, Y. Park, V. Asadchy, C. C. Wojcik, A. Dutt, and S. Fan, Nontrivial point-gap topology and non-hermitian skin effect in photonic crystals, *Physical Review B* **104**, 125416 (2021).
- [12] M. Reisenbauer, H. Rudolph, L. Egyed, K. Hornberger, A. V. Zasedatelev, M. Abuzarli, B. A. Stickler, and U. Delić, Non-hermitian dynamics and non-reciprocity of optically coupled nanoparticles, *Nature Physics* 10.1038/s41567-024-02589-8 (2024).
- [13] X. Piao and N. Park, Wave delocalization from clustering in two-dimensional non-hermitian disordered lattices, *ACS Photonics* **9**, 1655 (2022).
- [14] S. Longhi, Robust anderson transition in non-hermitian photonic quasicrystals, *Opt. Lett.* **49**, 1373 (2024).
- [15] S. Lieu, Topological phases in the non-hermitian su-schrieffer-heeger model, *Phys. Rev. B* **97**, 045106 (2018).
- [16] H. Shen, B. Zhen, and L. Fu, Topological band theory for non-hermitian hamiltonians, *Phys. Rev. Lett.* **120**, 146402 (2018).
- [17] L. Qian, W. Zhang, H. Sun, and X. Zhang, Non-abelian topological bound states in the continuum, *Phys. Rev. Lett.* **132**, 046601 (2024).
- [18] B. Wang, W. Liu, M. Zhao, J. Wang, Y. Zhang, A. Chen, F. Guan, X. Liu, L. Shi, and J. Zi, Generating optical vortex beams by momentum-space polarization vortices centred at bound states in the continuum, *Nature Photonics* **14**, 623 (2020).
- [19] Y. Chen, H. Deng, X. Sha, W. Chen, R. Wang, Y.-H. Chen, D. Wu, J. Chu, Y. S. Kivshar, S. Xiao, and C.-W. Qiu, Observation of intrinsic chiral bound states in the continuum, *Nature* **613**, 474 (2023).

- [20] B. Zhen, C. W. Hsu, L. Lu, A. D. Stone, and M. Soljačić, Topological nature of optical bound states in the continuum, *Phys. Rev. Lett.* **113**, 257401 (2014).
- [21] A. Cerjan, A. Raman, and S. Fan, Exceptional contours and band structure design in parity-time symmetric photonic crystals, *Phys. Rev. Lett.* **116**, 203902 (2016).
- [22] Q. Wang and Y. D. Chong, Non-hermitian photonic lattices: tutorial, *J. Opt. Soc. Am. B* **40**, 1443 (2023).
- [23] M. Liu, W. Chen, G. Hu, S. Fan, D. N. Christodoulides, C. Zhao, and C.-W. Qiu, Spectral phase singularity and topological behavior in perfect absorption, *Phys. Rev. B* **107**, L241403 (2023).
- [24] Y. D. Chong, L. Ge, H. Cao, and A. D. Stone, Coherent perfect absorbers: Time-reversed lasers, *Phys. Rev. Lett.* **105**, 053901 (2010).
- [25] M. S. Ergoktas, A. Kecebas, K. Despotelis, S. Soleymani, G. Bakan, A. Kocabas, A. Principi, S. Rotter, S. K. Ozdemir, and C. Kocabas, Localized thermal emission from topological interfaces, *Science* **384**, 1122 (2024), <https://www.science.org/doi/pdf/10.1126/science.ado0534>.
- [26] C. Guo, J. Li, M. Xiao, and S. Fan, Singular topology of scattering matrices, *Phys. Rev. B* **108**, 155418 (2023).
- [27] F. Wu, X. Qi, M. Qin, M. Luo, Y. Long, J. Wu, Y. Sun, H. Jiang, T. Liu, S. Xiao, and H. Chen, Momentum mismatch driven bound states in the continuum and ellipsometric phase singularities, *Phys. Rev. B* **109**, 085436 (2024).
- [28] R. Colom, E. Mikheeva, K. Achouri, J. Zuniga-Perez, N. Bonod, O. J. F. Martin, S. Burger, and P. Genevet, Crossing of the branch cut: The topological origin of a universal 2π -phase retardation in non-hermitian metasurfaces, *Laser & Photonics Reviews* **17**, 2200976 (2023), <https://onlinelibrary.wiley.com/doi/pdf/10.1002/lpor.202200976>.
- [29] J. K. Asbóth, L. Oroszlány, and A. Pályi, *A Short Course on Topological Insulators*, Lecture Notes in Physics, Vol. 919 (Springer International Publishing, 2016).
- [30] J. C. G. Henriques, T. G. Rappoport, Y. V. Bludov, M. I. Vasilevskiy, and N. M. R. Peres, Topological photonic tamm states and the su-schrieffer-heeger model, *Phys. Rev. A* **101**, 043811 (2020).
- [31] W. P. Su, J. R. Schrieffer, and A. J. Heeger, Solitons in polyacetylene, *Phys. Rev. Lett.* **42**, 1698 (1979).

- [32] N. D. Mermin, The topological theory of defects in ordered media, *Rev. Mod. Phys.* **51**, 591 (1979).
- [33] M. J. P. Gingras and D. A. Huse, Topological defects in the random-field xy model and the pinned vortex lattice to vortex glass transition in type-ii superconductors, *Phys. Rev. B* **53**, 15193 (1996).
- [34] M. Kang, T. Liu, C. T. Chan, and M. Xiao, Applications of bound states in the continuum in photonics, *Nature Reviews Physics* **5**, 659 (2023).